optical filter). At all temperatures, recovery is >99%.

Quantitative analysis of mixtures of **2a** and **2b** can be effected by ^1H NMR because the regions of aliphatic and vinyl absorption are sufficiently well separated on the 300-MHz instrument, owing to the large ^1H-^{13}C coupling constants. Aliphatic hydrogen atoms at C3 and C4 in **2a** are a narrow triplet at 2.61 (T_1 = 1.73 ± 0.07 s) whereas in **2b** they are seen as widely separated doublets at 2.40 and 2.81 (T_1 = 1.23 ± 0.07 s). Conversely, the *Z* and *E* vinyl hydrogen atoms in **2a** appear as a pair of widely separated doublets at 5.00 and 5.52 (T_1 = 1.08 ± 0.07 s) and 4.70 and 5.22 (T_1 = 1.08 ± 0.07 s), respectively. In **2b**, they appear as the pair of narrow doublets centered at 5.27 (T_1 = 1.80 ± 0.07 s) and 4.96 (T_1 = 1.66 ± 0.07 s), respectively.

To ensure accuracy of integration, spectra are recorded with a pulse interval of 9.0 s, corresponding to five times the longest value of T_1 shown by the protons of interest. In practice, four areas are measured in the vinyl region by integration: I_1, H_Z(**2a**) at 5.52; I_2, [H_E(**2a**) + H_Z(**2b**)] at 5.22 and 5.27, respectively; I_3, [H_Z(**2a**) + H_E(**2b**)] at 5.00 and 4.96, respectively; and I_4, H_E(**2a**) at 4.77. Three areas are measured in the aliphatic region: I_5, H_a(**2b**) at 2.81; I_6, H_a(**2a**) at 2.61; and I_7, H_a(**2b**) at 2.40.

Correction is made for the fact that each methylene group in the starting material, dibenzoylethane, is 98.90% ^{12}C and 1.10% ^{13}C, whereas the methyltriphenylphosphonium ylide is 99.42% ^{13}C and 0.58% ^{12}C. The result is four distinct β-phenylallyl groups: *A*(^{13}C-1), 98.326% and *B*-(^{13}C-3), 0.006% (interchangeable on Cope rearrangement); and *C*(^{13}C-1, ^{13}C-3), 1.094% and *D*(only ^{12}C), 0.574% (neither altered on Cope rearrangement).

Ratios of **2a**/**2b** (A/B) are calculated in three different ways (they agree within 0.7%) and are averaged for use in the calculations of specific rate constants (the sums, [H_Z(**2a**) + H_Z(**2b**)], [H_E(**2a**) + H_E(**2b**)], and [H_a(**2a**) + H_a(**2b**)], are normalized to 100): (i) area H_Z(**2a**) = $2I_1$ = *A* + *C* and area H_Z(**2b**) = $I_2 - I_4$ = *B* + *D*, whence $A/B = (2I_1 - 1.094)/(I_2 - I_4 - 0.574)$; (ii) area H_E(**2a**) = $2I_4$ = *A* + *C* and area H_E(**2b**) = $I_3 - I_1$ = *B* + *D*, whence $A/B = (2I_4 - 1.094)/(I_3 - I_1 - 0.574)$; (iii) area H_a(**2a**) = I_6 = *A* + *D* and area H_a(**2b**) = $I_5 + I_7$ = *B* + *C*, whence $A/B = (I_6 - 0.574)/(I_5 + I_7 - 1.094)$.

Results are given in Table VII. Rate and equilibrium constants are optimized simultaneously by the nonlinear least-squares S curve fitting of observed data to the standard kinetic equation for reversible, first-order reactions. The long-time points are not included because the amount of byproduct is no longer negligible.

Acknowledgment. This material is based upon work supported by the National Science Foundation under Grant CHE-86-18451 and in part (T.K.) by PHS Grant 1 R0 1 CA41325-01 awarded by the National Cancer Institute, DHHS. Thanks goes to the National Institutes of Health for Instrumentation Grant 1 S10 RR01748-01A1 toward the purchase of a Bruker AM300 NMR spectrometer. We thank the German Research Society and the Chemical Industry Fund for financial support. We are grateful to Dr. Tommy Liljefors, University of Lund, Sweden, for having calculated the enthalpy of formation of **4** with the inclusion of electrostatic interaction.

Registry No. 2, 7283-49-0; **2a**, 72316-06-4; **3**, 27905-65-3; **4**, 94383-67-2; *endo*-**4**, 125024-89-7; *exo*-**4**, 125024-90-0; dibenzoylethane, 495-71-6; *meso*-2,5-diphenylhexane, 21451-75-2; *rac*-2,5-diphenylhexane, 21451-42-3; *meso*-2,6-diphenylheptane, 125024-87-5; *rac*-2,6-diphenylheptane, 125024-88-6; bicyclo[3.2.0]heptane, 278-07-9; 2-phenylhexa-1,5-diene, 7399-52-2; 1,4-diphenylhexa-1,5-diene, 69693-35-2; *meso*-3,4-diphenylhexa-1,5-diene, 33788-14-6; *rac*-3,4-diphenylhexa-1,5-diene, 33788-15-7; 3-phenylhexa-1,5-diene, 1076-66-0; 2,4-diphenylhexa-1,5-diene, 63779-63-5.

Factors Controlling the Synchronous versus Asynchronous Mechanism of the Cope Rearrangement

Michael Bearpark,[†] Fernando Bernardi,*[,‡] Massimo Olivucci,[†] and Michael A. Robb*[,†]

Contribution from the Dipartimento di Chimica, "G. Ciamician", dell'Università di Bologna, Via Selmi 2, 40126 Bologna, Italy, and the Department of Chemistry, King's College, London, Strand, London WC2R 2LS, U.K. *Received May 22, 1989*

Abstract: MC-SCF potential surfaces for the Cope rearrangement of 1,5-hexadiene have been modeled by using a valence bond (VB) scheme parametrized with effective Hamiltonian methods. It is demonstrated that the mechanistic preference for a synchronous mechanism with an aromatic transition state versus an asynchronous mechanism with a biradicaloid intermediate is controlled by two factors: (i) the stability of the long bond in the Dewar VB structure and (ii) the softness of the Coulomb interactions between the terminal methylenes of the allylic fragments. Thus, the mechanism may be strongly affected by substituents.

I. Introduction

There has been a controversy concerning the mechanism of the chair Cope[1] rearrangement for many years. Conflicting experimental and theoretical studies[2-20] provide evidence to support both a synchronous mechanism with an "aromatic" transition state (Scheme I) and a biradical mechanism involving a biradical intermediate (Scheme II). From a theoretical point of view, in multibond reactions it is essential to use a wave function where the possibility of biradical and aromatic transition states can be treated with a balanced level of accuracy. Thus, the MC-SCF results of Morokuma et al.[20] on the Cope rearrangement of the "model" reaction of 1,5-hexadiene are very convincing and provide reliable evidence that the lowest energy pathway for the model reaction is the synchronous one with the biradical intermediate

Scheme I

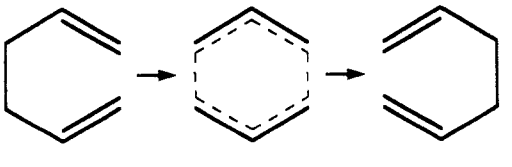

Scheme II

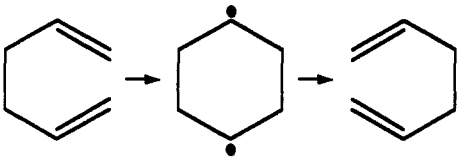

lying 22 kcal mol^{-1} higher in energy than the synchronous transition state.

[†] King's College, London.
[‡] Università di Bologna.

0002-7863/90/1512-1732$02.50/0

Chart I

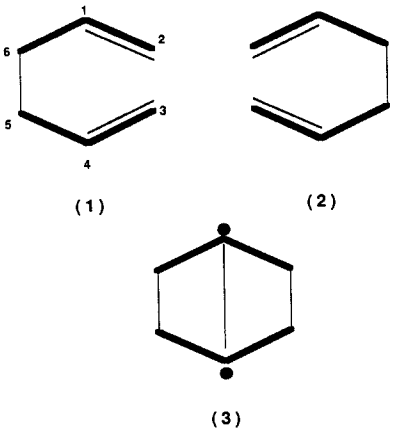

However, such calculations say nothing about the factors that control the mechanistic preference. Our objective in this paper is to show why the model reaction has the mechanism it has by using a valence bond (VB) analysis[21] of an MC-SCF wave function similar to that used by Morokuma et al.[20] Since it is very expensive to study even the model reaction with ab initio methods, the "understanding" provided by a VB analysis of the MC-SCF results for the model reaction can give some insight as to why a broad spectrum of experimental and theoretical results appear to be obtained for this reaction.

In recent work[21] we have shown how an MC-SCF wave function can be transformed into a simple VB wave function via the construction of an effective Hamiltonian.[22] By virtue of the use of an effective Hamiltonian technique, the VB model obtained in this way reproduces the MC-SCF energy *exactly*. The VB Hamiltonian itself (a Heisenberg spin Hamiltonian)[22] is a simple function of Coulomb integrals (Q_{ij}) and exchange integrals (K_{ij}) that depend on the distance between the sites of the "active" atomic orbitals (i.e., those involved in bond making and breaking). For the purposes of *qualitative* interpretation, these integrals can be assumed to have the same form as the Heitler–London treatment of H_2 as shown in eq 1 and 2. Here i,j are active orbitals, $[ii|jj]$

$$Q_{ij} = Q_C + [ii|jj] + \langle i|h|i\rangle + \langle j|h|j\rangle \quad (1)$$

$$K_{ij} = [ij|ij] + 2s_{ij}\langle i|h|j\rangle \quad (2)$$

and $[ij|ij]$ are the usual two-electron repulsion integrals (negligible until the distance between the sites of orbitals i and j becomes small), $\langle i|h|i\rangle/\langle i|h|j\rangle$ are the usual one-electron integrals (which will be dominated by the nuclear electron attraction term and are thus negative), and s_{ij} are overlaps between the nonorthogonal AO. The term Q_C contains the effect of the closed-shell "core" and contains effects due to nonbonded repulsions and steric effects. The *numerical* values of these integrals are not dependent on this approximation, but rather are extracted from an effective Hamiltonian computation and fitted to simple functions of the interatomic distances (aside from "more than two electron" integrals, which are handled as discussed in ref 21). Thus, the VB Hamiltonian is parametrized to reproduce the results of an MC-SCF computation rather than experimental data. (For a general review of this type of approach the reader is referred to the review paper of Durand and Malrieu.[22]) The accuracy of this approach is limited only by the sophistication of the fitting of the Q_{ij} and K_{ij}, and because we are interested in qualitative interpretation, we have used only very simple functions of interatomic distances.

For the Cope rearrangement we have six active orbitals corresponding to the p^π atomic orbitals of the allylic fragments. The VB wave function corresponds to the usual five VB structures for a six-orbital six-electron problem. For the Cope rearrangement, we should expect that only the three structures (two Kekule and one Dewar structure) shown in Chart I may be important. A *diabatic surface*, in our model, is defined as the energy of one of the VB structures[21] and corresponds to the energy of a specific bonding situation. Accordingly, energy of the diabatic surface associated with a given structure is given simply by the relevant VB energy expression as

$$E = Q + \sum_{ij}^{\text{spin-coupled pairs}} K_{ij} - \tfrac{1}{2}\sum_{kl}^{\text{uncoupled pairs}} K_{kl} \quad (3)$$

(Equation 3 is the general energy expression for a VB structure in the Rumer basis. In ref 21 we have used a different spin-coupling scheme based upon orthogonal spin-coupled functions.) Thus, the energy of the various VB structures that interact to give the MC-SCF surface is easily computed. An examination of the behavior of the diabatic surfaces given some insight as to the origin of the reaction barriers. The behavior of the diabatic surfaces themselves and the total energy can thus be easily rationalized in terms of the Q_{ij} and K_{ij}, which the simple functions of the interatomic distances and the overlap.

II. Parametrization of the VB Hamiltonian

We now give the essential details of the parametrization of the VB Hamiltonian used to model the MC-SCF results. From the outset we must emphasize that our objective is to obtain a global representation of the surface of this reaction that is in qualitative agreement with the MC-SCF results of ref 17 and 18 at the STO 3G and 3-21G levels. In order to interpret the results in a chemical way, we have used a simple physically motivated model for the parameters and this must obviously limit the accuracy that can be achieved.

There are two sides to the problem. On the one hand, using the effective Hamiltonian methods we have described in ref 21 one can obtain a numerical Heisenberg spin Hamiltonian in the space of the VB determinants that will reproduce the MC-SCF energies exactly. On the other hand, this Hamiltonian is to be modeled with Coulomb and exchange parameters that are implicitly assumed to have the form given by eq 1 and 2. However, as discussed in detail in ref 21, the exact numerical effective Hamiltonian deviates from the Heisenberg form because of more than two electron integrals. This occurs because the numerical Heisenberg effective Hamiltonian contains the effect of powers of orbital overlap integrals higher than 1. In order to use a simple parametrization, these more than two electron effects must be averaged. An alternative strategy would be to parametrize simple two or four active electron model systems where the problem of more than two electron integrals does not occur[21] and transfer these parameters. As we shall discuss below, this strategy yields a parametrization of the model Hamiltonian that reproduces the behavior of the averaged parameters in the numerical effective

(1) Levy, H.; Cope, A. C. *J. Am. Chem. Soc.* **1944**, *66*, 1684.
(2) Doering, W. v. E.; Roth, W. R. *Tetrahedron* **1962**, *18*, 67.
(3) Fukui, K.; Fusimoto, H. *Tetrahedron Lett.* **1966**, 251.
(4) Hill, R. K.; Gilman, N. W. *Chem. Commun.* **1967**, 620.
(5) Simonetta, M.; Favini, G.; Mariani, G.; Gramaccioni, P. *J. Am. Chem. Soc.* **1968**, *90*, 1280.
(6) Humski, K.; Sunko, D. E. *J. Am. Chem. Soc.* **1970**, *92*, 6534.
(7) Brown, A.; Dewar, M. J. S.; Schoeller, W. *J. Am. Chem. Soc.* **1970**, *92*, 5516.
(8) Doering, W. v. E.; Toscano, V. G.; Beasley, G. H. *Tetrahedron* **1971**, *27*, 5299.
(9) Goldstein, M. J.; Benzon, M. S. *J. Am. Chem. Soc.* **1972**, *94*, 5119, 7147, 7149.
(10) Dewar, M. J. S.; Wade, L. E. *J. Am. Chem. Soc.* **1973**, *95*, 291.
(11) McIver, J. W.; Komornicki, A. *J. Am. Chem. Soc.* **1976**, *98*, 4553.
(12) Dewar, M. J. S.; Ford, G. P.; Mackee, M. L.; Rzepa, H. S.; Wade, L. E. *J. Am. Chem. Soc.* **1977**, *99*, 5069.
(13) Rossi, M.; King, K. D.; Golden, D. M. *J. Am. Chem. Soc.* **1979**, *101*, 1223.
(14) Gajewski, J. J.; Conrad, N. D. *J. Am. Chem. Soc.* **1979**, *101*, 6693.
(15) Gajewski, J. J. *Hydrocarbon Thermal Isomerization*; Academic Press: New York, 1981; pp 166–176.
(16) Doering, W. v. E. *Proc. Natl. Acad. Sci. U.S.A.* **1981**, *78*, 5279.
(17) Osamura, Y.; Kato, S.; Morokuma, K.; Feller, D.; Davidson, E. R.; Borden, W. T. *J. Am. Chem. Soc.* **1984**, *106*, 3362.
(18) Dewar, M. J. S.; Healy, E. F. *Chem. Phys. Lett.* **1987**, *141*, 521.
(19) Dewar, M. J. S.; Jie, C. *J. Am. Chem. Soc.* **1987**, *109*, 5983.
(20) Morokuma, K.; Borden, W. T.; Hrovat, D. A. *J. Am. Chem. Soc.* **1988**, *110*, 4474.
(21) Bernardi, F.; Olivucci, M.; McDouall, J. J. W.; Robb, M. A. *J. Chem. Phys.* **1988**, *89*, 6365.
(22) Durand, P.; Malrieu, J. P. *Adv. Chem. Phys.* **1987**, *67*, 321–412.

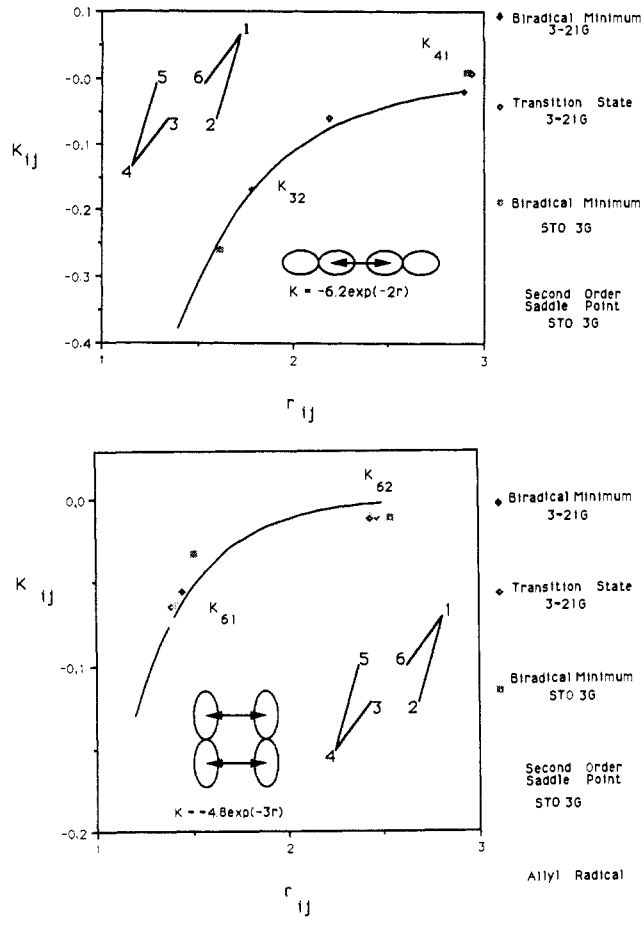

Figure 1. Parametization of K_{ij} for (a, top) p^{σ}–p^{σ} and (b, bottom) p^{π}–p^{π} interactions. The solid curve shows the behavior of the functional form used to generate the global surfaces. The individual points represent averaged K_{ij} obtained from numerical effective Hamiltonian computations in the 3-21G six-orbital six-electron CAS space.

Hamiltonian quite well and is physically appealing as well. This procedure proves to be adequate to give a global representation of the surface that is qualitatively correct.

From the form of eq 1 and 2 it is clear that we require a functional form for the interaction (Q_{ij} and K_{ij}) of a pair of p orbitals on each site i and j. In order to keep our model simple, we shall assume that only two types of p–p exchange (K_{ij}) interaction are possible: a p^{π}–p^{π} (e.g., 6–1 or 6–2 in Chart I) or a p^{σ}–p^{σ} (e.g., 3–2 or 4–1 in Chart I). Since this effect should be dominated by overlap effects, the functional form used was chosen to be

$$K_{ij} = a \exp(br_{ij}) \tag{4}$$

The parameters a and b were estimated from MC-SCF computations on the π system of ethylene (for the p^{π}–p^{π} $a = -4.8$, $b = 3$) and from four-orbital four-electron MC-SCF computations on the trans addition of two ethylene molecules to form the trans tetramethylene biradical (for the p^{σ}–p^{σ} $a = -6.2$, $b = 2$). This parametrization reproduces the trends of the averaged values of the K_{ij} from the numerical Heisenberg effective Hamiltonians at various critical points of the Cope rearrangement as shown in Figure 1. Note that the K_{ij}s are not sensitive to the basis set used.

The Coulomb terms Q_{ij} present more subtle difficulties. From a numerical computation of the full six-electron Heisenberg Hamiltonian one obtains only the total contribution from all the Q_{ij}. Thus, in this case one is forced to parametrize the Q_{ij} from simpler model systems. For the p^{π}–p^{*} between bonded (via the σ framework) atoms we obtained Q_{ij} from MC-SCF/4-31G computations on the model system ethylene. Thus, we use a simple Morse potential of the form

$$Q_{ij} = D_e[1 - \exp(-a(r_{ij} - r_0))]^2 \tag{5}$$

Chart II

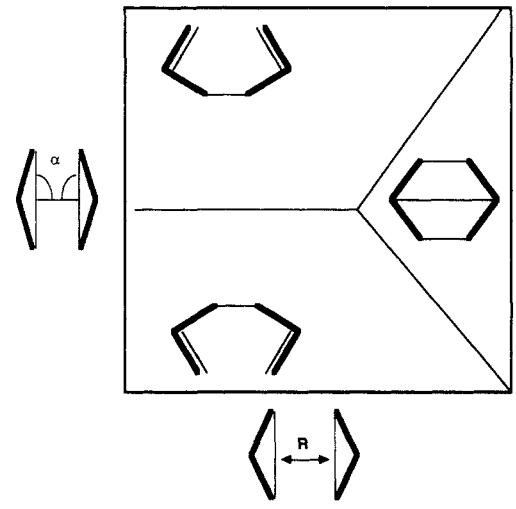

with $D_e = 0.40021E_h$, $a = 0.94$, and $r_0 = 2.645a_0$. The Coulomb term for interactions that do not have a σ framework is expected to be dominated by the nonbonded repulsions in Q_C, and thus a generalized Lennard-Jones potential has been used.

$$Q_{ij} = n\epsilon/(n - m)\{m/n[r_0/r_{ij}]^n - [r_0/r_{ij}]^m\} \tag{6}$$

For all interactions except those involved in the making/breaking of the σ bonds 2–3 and 5–6 we have used standard values of m, n, ϵ, and r_0 ($r_0 = 7.18a_0$, $\epsilon = 0.0000699E_h$, $n = 12$, $m = 6$). For the interactions involved in the making/breaking of the σ bonds 2–3 and 5–6, we have reparametrized the Lennard-Jones potential using data obtained from four-orbital four-electron MC-SCF computations (at the STO-3G and 4-31G levels) on the trans addition of two ethylene molecules to form the tetramethylene biradical. The parameters are discussed in detail in the next section. We have tacitly assumed that the differences in the potential energy surface of the Cope rearrangement at 4-31G and 3-21G are unimportant from a qualitative point of view (i.e., the surface topology will be the same).

We must emphasize that the parametrization just outlined is very simple and one must be content with reproducing only the qualitative features of the MC-SCF surface of the Cope rearrangement. Nevertheless, this same type of parametrization has successfully reproduced the surface topology of our previous MC-SCF computations on the 2 + 2 cycloaddition of two ethylene molecules, the Diels–Alder reaction, the electrocyclic reaction of butadiene, and the 1,3 dipolar cycloaddition of acetylene and fulminic acid. It has the advantage that the physical origin of each parameter is clear and thus we have the possibility to examine the effects of perturbations in these parameters, which we now exploit.

III. Results and Discussion

It is convenient to discuss the mechanism of the Cope rearrangement in a subspace of two geometric variables R (the interallylic distance) and α (an asymmetric distortion leading to 1,5-hexadiene) as shown in Chart II. In Chart II we have delineated three regions of interest corresponding to two 1,5-hexadiene minima and the biradicaloid minimum indicated by the structure with the "long bond". In Figure 2, we show the corresponding potential energy surface for the Cope rearrangement obtained by using the VB model computation (with the Q_{ij} parametrized at the 4-31G level as described previously). The X axis (top left to bottom right diagonal) corresponds to the interallylic distance (R in Chart II) and the Y axis (top right to bottom left diagonal) corresponds to an asymmetric distortion leading to 1,5-hexadiene (i.e., the angle α illustrated in Chart II, which corresponds to the transition vector for the aromatic transition state given by Morokuma et al.[20]). The remaining geometrical variables have been interpolated. In Figure 2 we see the topological

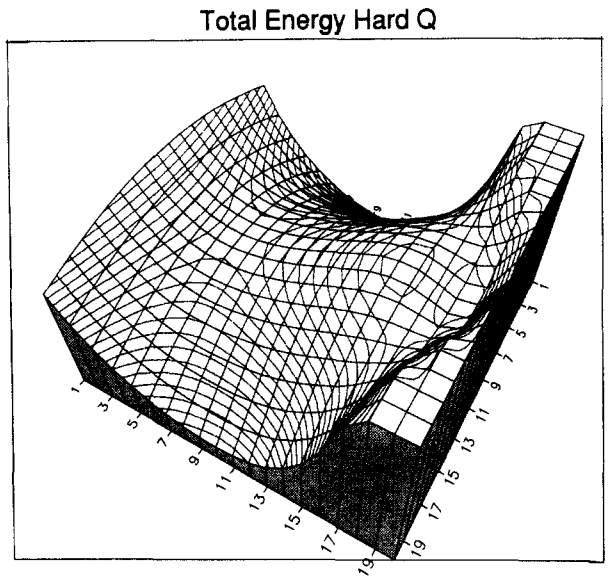

Figure 2. Potential energy surface (from VB model parametrized at the 4-31G level) for the Cope rearrangement of 1,5-hexadiene. The X axis (diagonal top left to bottom right) is the interallylic distance R and the Y axis (diagonal top right to bottom left) is the angle α defined in Chart II. Each division on the X axis corresponds to an increment of −0.04 Å and the first division corresponds to R = 2.55 Å. Each division on the Y axis corresponds to an increment of 1° and the first division corresponds to α = 80°. The remaining geometrical parameters have been interpolated as a function of R from the MC-SCF optimized geometries.

features corresponding to the synchronous transition state that connects the two 1,5-hexadiene minima and the shallow biradicaloid minimum. One can also observe the two biradicaloid transition structures that must connect the 1,5-hexadiene minima and the biradical minimum. The synchronous transition state and the biradicaloid minimum have been completely characterized by Morokuma et al.[20] and the biradicaloid transition states have been characterized in semiempirical work.[12] However, there is an additional topological feature, a local maximum, that separates the aromatic transition state and the biradical minumum that must exist but has not been characterized in theoretical computations. Of course, the surface in Figure 2 gives the synchronous transition structure at a lower energy than the biradical minimum because the surface has been explicitly parametrized to reproduce the MC-SCF results. Given the simplicity of the model used to generate these surfaces, we cannot expect better than general qualitative agreement with the MC-SCF results of Morokuma et al.[20] However, as we shall now demonstrate, the advantage of the simple model lies in the fact that we can make small perturbations on the parameters in the model in order to understand the origin of the mechanistic preference.

The origin of the topological features of the potential energy surface is clearly evident from Figure 3, where we have plotted the lowest energy sheet for the three diabatic surfaces shown in Chart I and illustrated schematically in Chart II. The aromatic transition state that corresponds to the synchronous pathway lies on the ridge of the "seam" of intersection of the two Kekule structures (**1** and **2** in Chart I), as it must by symmetry. The biradical minimum lies in a well on the surface for the Dewar structure (**3** in Chart I). The asymmetric transition states leading to the biradical minimum lie on the seam of intersection between a Kekule structure and a Dewar structure as expected. Finally, the local maximum corresponds to the intersection of the three diabatics associated with Chart I.

The behavior of the three diabatic surfaces is easily rationalized qualitatively. The energy of each of the Kekule structures is weakly repulsive as R is decreased (holding α fixed). In eq 3 for structure **1**, K_{12}, K_{34}, and K_{56} (Chart I) will occur with a positive sign and are thus their contribution to the energy is stabilizing (since K_{ij} is negative), the remaining K_{ij} will occur with a negative sign and are thus their contribution to the energy is destablizing,

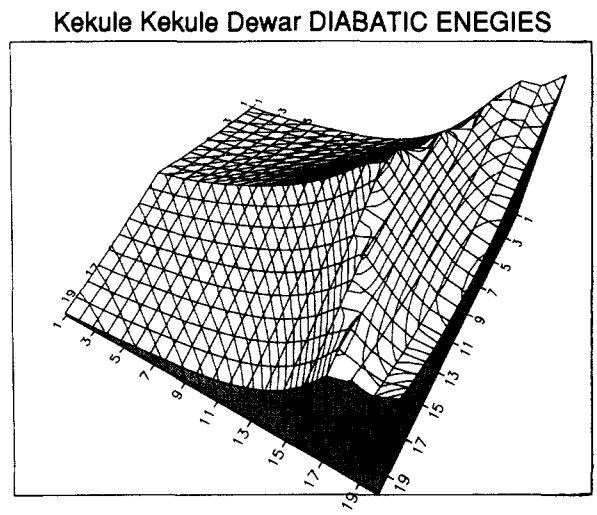

Figure 3. Diabatic surfaces (computed by using eq 3) for the lowest energy sheet for each of the three structures shown in Chart I. The grid is the same as for Figure 2.

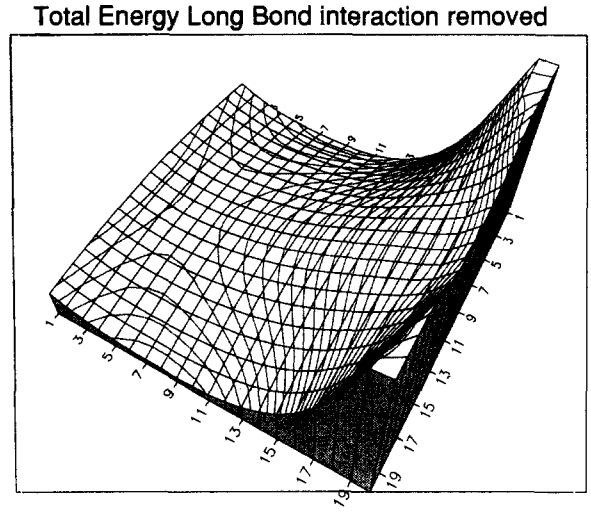

Figure 4. Potential energy surface (from VB model parametrized at the 4-31G level) for the Cope rearrangement of 1,5-hexadiene where the long-bond interaction K_{14} has been turned off. The grid is the same as for Figure 2.

and of course, Q is repulsive. Thus, the increase of the magnitude of K_{56} as R is decreased is offset by the increase of K_{23}, which occurs in the energy expression with the opposite sign with the result that the repulsive nature of Q dominates. Similarly, as α is changed (with R fixed so that Q is almost constant) on moving from 1,5-hexadiene to a symmetric structure, the energy is repulsive because the magnitude of K_{56} will decrease and the magnitude of K_{23} will increase but the contribution to the energy from K_{56} is stabilizing while the contribution to the energy from K_{23} is destabilizing. In contrast, as R is decreased in the region of the biradical minimum, the energy of the Dewar structure is strongly attractive because K_{23}, K_{14}, and K_{56} all occur in eq 3 with a positive sign and thus their contribution to the energy is stabilizing.

We can now *experiment* with the Coulomb and exchange parameters in the definition of our VB model to attempt to understand the reasons for the preference for the synchronous pathway as opposed to the biradical structure.

First one may examine the stability of the biradicaloid Dewar structure by "turning off" the biradical long-bond interaction K_{14} (for atom numbering see Chart I) in the VB model. The corresponding surface is shown in Figure 4. Notice that the biradical minimum disappears completely. At first this seems surprising since the C_1–C_4 distance is 2.89 Å at the biradicaloid minimum, and the explanation is rather subtle. The contribution of the K_{14}

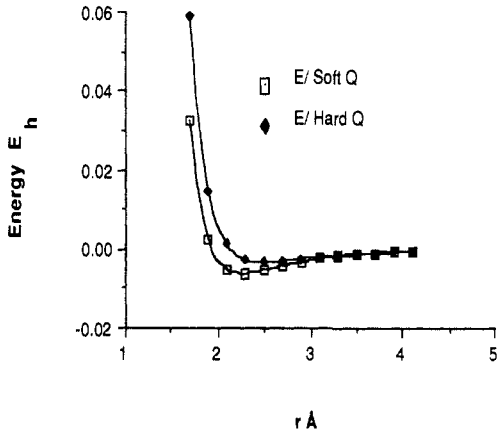

Figure 5. Behavior of Q_{65}/Q_{32} for hard and soft Q.

integral is destabilizing at the geometry of the synchronous transition structure because at this geometry the wave function is dominated by the two Kekule structures and K_{14} occurs with a negative sign when eq 3 is evaluated for a Kekule structure. In contrast, the contribution from the K_{14} integral is stabilizing at the geometry of the biradicaloid minimum where the wave function is dominated by the Dewar structure because K_{14} occurs with a positive sign in the evaluation of the energy using eq 3. Because the long-bond exchange interaction effects the energy of the synchronous transition structure and the energy of the Dewar structure in the opposite way, a very small change in the strength of this interaction has a dramatic effect on the potential surface topology. We have thus demonstrated that the biradical minimum is in fact biradicaloid with a "long" bond that accounts for the stability of this species.

Let us turn now to the effect of the *Coulomb energy*. As we shall now show, the topology of the potential surface is controlled by the nature of the interallylic terms in Q. As discussed previously, the ab initio MC-SCF Q_{ij} values for Q_{65} and Q_{32} fit reasonably well to a generalized Lennard-Jones potential of the form given in eq 6. In order to fit the Q_{65} and Q_{32} to a VB model that reproduces MC-SCF computations, the potential must be modified from the form normally used for nonpolar atoms (m = 12, n = 6). In particular, the well depth ϵ is deeper and occurs at shorter range, and in addition, the repulsive part ($[r_0/r]^n$) is less steep. Both these effects arise because of the electron–nuclear attraction terms ($\langle i|h|i\rangle$) in eq 2. For Q_{65} and Q_{32} the parameters for 4-31G basis sets are $\epsilon = 0.000325E_h$, r_0 = 2.50 Å, n = 6.7, and m = 6.0. This parametrization was used in Figure 2. We can now experiment by making Q_{65} and Q_{32} "softer" by setting r_0 to a smaller distance and increasing the well depth. In Figure 5 we show the curve obtained by setting $\epsilon = 0.000606E_h$ and r_0 = 2.26 Å so that the minimum in Q_{65} and Q_{32} occurs at a shorter interfragment distance and is deeper. The two forms of Q_{65}/Q_{23} are illustrated in Figure 5. The surface that results when Q_{65}/Q_{32} have this soft form is shown in Figure 6. Now, the synchronous (aromatic) transition state shows itself only as a shoulder (which would be impossible to locate with standard geometry optimization algorithms) and the biradicaloid minimum lies in a deep well. Thus, one can conclude that the stability of the biradical region of the surface is delicately controlled by the nature of the Coulomb interactions Q_{65} and Q_{32}. If this interaction is soft (small r_0, large ϵ) the biradical mechanism may become dominant. If this interaction is hard (large r_0, small ϵ), the synchronous mechanism may become dominant. Clearly, Q will be affected by substituents and one may expect a range of mechanisms that depends upon the hardness or softness of Q.

Finally we note that this same term also explains the basis set dependence of the MC-SCF results (compare ref 17 and 20) and delicately controls the preference of the synchronous versus asynchronous pathways. In fact, the values of $\epsilon = 0.000606E_h$ and r_0 = 2.26 Å and Q_{65} and Q_{32} are those we obtain with the STO 3G basis and Figure 6 is in qualitative agreement with the MC-SCF results obtained in ref 17 at the STO-3G level. Thus, the

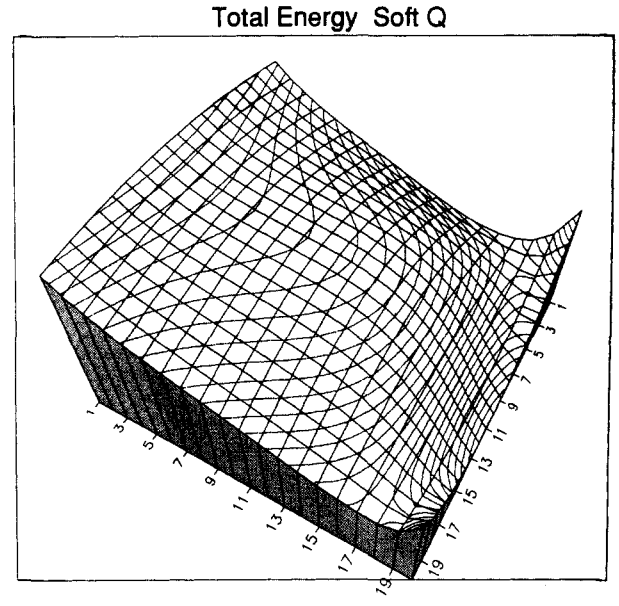

Figure 6. Potential energy surface for the Cope rearrangement of 1,5-hexadiene for a soft Q ($\epsilon = 0.000606E_h$ and r_0 = 2.26 Å in eq 4). The X axis and Y axis are defined as in Figure 2.

minimum in Q_{65} and Q_{32} occurs at a larger interfragment distance and is shallower for the 4-31G basis ("hard Q") compared to the STO-3G basis ("soft Q"). This observation gives additional confidence to the predictions obtained with our simple VB model.

IV. Conclusions

We have applied a simple VB model, parametrized to reproduce the results of MC-SCF computations, for the "model" Cope rearrangements. This global simulation provides a qualitative summary of much more detailed MC-SCF computations. In particular, we obtain insight into three questions. What is the origin of the various possible transition states for the competing mechanisms? What physical effects (Coulomb and exchange interactions) control the surface topology and thus the balance between aromatic and biradicaloid mechanisms? Why does the mechanism of the reaction appear to be very sensitive to substituents? The answers to such questions are not obtained from the MC-SCF calculations of energetics and equilibrium/transition structure geometries themselves.

The origin of the various transition structures is easily appreciated within a VB model. Each of the transition structures lies on the "ridge" of intersection between two diabatic surfaces. Thus, the barrier in each case is associated with the electronic rearrangement associated with a change of spin coupling from one bonding situation to another. The transition state that corresponds to the aromatic mechanism (synchronous pathway) corresponds to the change of spin coupling from one Kekule structure to another Kekule structure, while the transition structures for the biradicaloid (asynchronous) pathway correspond to a change from Kekule to Dewar structures. The three minima (reactants/product and the biradical intermediate) are each associated with a minimum on one of the three diabatic surfaces. Finally, the local maximum on the potential energy surface corresponds to the intersection of three diabatic surfaces. Thus, topology of the global potential energy surface can be rationalized in terms of three VB structures.

Using the VB model, we have identified two key features that control the topology of the potential surface and (i) the "hardness" or "softness" of the Coulomb integrals Q_{65} and Q_{32} between the centers where bonds are being broken and formed and (ii) the biradical long-bond interaction K_{14}. These two features in turn provide some rationalization of the experimental fact that the mechanism appears to be sensitive to substiuent effects.

First, if the Q_{65} and Q_{32} are made soft, then the biradical region becomes stabilized. If Q is made "harder" the synchronous pathway becomes favored. One could make Q_{65} and Q_{32} "hard",

for example, through steric effects (which will increase the Q_C contribution) via the presence of bulky groups at the terminal allylic methylene centers and thus force a synchronous mechanism.

Second, the surface topology is influenced strongly by the long-bond interaction K_{14}. We have shown that if the long-bond interaction K_{14} is turned off, the biradical region disappears. Thus, the presence of a substituent at sites 1 or 4 that enhances this effect will force a biradicaloid mechanism. Dewar and Wade[10] have shown that phenyl substitution at the positions 1 and 4 increases the rate by a factor of 2000, in agreement with this observation.

Registry No. 1,5-Hexadiene, 592-42-7.

Mechanism of Ground-State-Forbidden Photochemical Pericyclic Reactions: Evidence for Real Conical Intersections

Fernando Bernardi,*[1a] Sushovan De,[1b] Massimo Olivucci,[1b] and Michael A. Robb*[1b]

Contribution from the Dipartimento di Chimica, "G. Ciamician", dell'Universita di Bologna, Via Selmi 2, 40126 Bologna, Italy, and the Department of Chemistry, King's College, London, Strand, London WC2R 2LS, U.K. *Received May 31, 1989*

Abstract: The presence of a conical intersection between the S_0 and S_1 surfaces for ground-state-forbidden photochemical pericyclic reactions is demonstrated by using results from an effective (valence bond) Hamiltonian and MC-SCF computations. The existence of such topological features is an important feature in the mechanism since it permits a fully efficient return to S_0 from the S_1 excited state. An example is presented for the 2 + 2 cycloaddition reaction of two ethylene molecules and the electrocyclic reaction of *cis*-butadiene.

I. Introduction

Pericyclic reactions, which are ground-state-forbidden (in the Woodward–Hoffmann scheme), are assumed to be excited-state-allowed in S_1 because the surface topology of S_1 is assumed to possess a minimum that corresponds to a diradicaloid structure that has approximately the same geometry as the "antiaromatic" transition state on S_0. Thus, the central feature in the mechanism of an excited-state pericyclic reaction is usually assumed to be the existence of suitable surface crossing (a funnel) that allows for the occurrence of a radiationless jump from S_1 to S_0. (For a good discussion of these points the reader is referred to ref 2 and 3). The decay probability P from S_1 to S_0 can be approximated by the Landau Zener formula (see the discussion of Salem[3] or Tully and Preston[4]):

$$P = \exp -\pi^2 g^2 / h\nu\, \delta s \qquad (1)$$

where ν is the nuclear velocity along the reaction coordinate, g is the energy gap at the avoided crossing, and δs is the difference in slopes between the intersecting "diabatic" states. Clearly, the larger the value of g the smaller is P. The surfaces S_1 and S_0 are assumed to avoid each other and it is this gap g that controls this reaction.

In contrast to the preceding discussion, if the S_0 and S_1 states actually touch at the funnel geometry (in a conical intersection[5]), the return to S_0 will be fully efficient since the return to S_0 occurs as soon as the funnel is reached. As a consequence, the rate of the reaction will not be controlled by the gap g between the S_0 and S_1 surfaces but will be controlled by the usual topological features of either the ground- or excited-state surfaces (e.g., a transition state arising from an S_1/S_2 avoided crossing on the excited surface). It is widely recognized that such conical intersections do frequently occur, and the purpose of this article is to demonstrate this for two "textbook" pericyclic reactions, the 2 + 2 cycloaddition of two ethylene molecules and the electrocyclic ring closure of *cis*-butadiene.

Scheme I

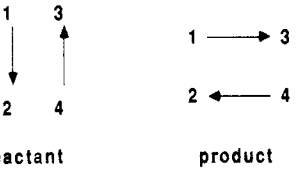

Recently, we have shown[6] how an MC-SCF wave function can be transformed to valence bond (VB) space. (For a discussion of VB theory as used in this paper, the reader is referred to ref 7 and 8.) We now give a simple discussion of how such a conical intersection can arise in the language of VB theory and then demonstrate using the methods discussed in ref 6 that such a topological feature actually arises for the two reactions.

We shall illustrate our discussion using the classical example of the 2 + 2 reaction of two ethylene molecules. In VB theory we can represent (at the simplest level) the ground and "valence" excited states of two ethylene molecules using two VB structures characteristic of the spin coupling of the reactant and products as shown in Scheme I. Using a two-level secular equation, taking one reference wave function as the reactant and the other as the

(1) (a) Dipartimento G. Ciamician, dell'Universita di Bologna. (b) King's College, London.

(2) (a) Turro, N. J. *Modern Molecular Photochemistry*; Benjamin Publishing: Reading, MA, 1978. (b) Michl, J.; Bonacic-Kotecky, V. *Electronic Aspects of Organic Photochemistry*; Wiley, New York, 1989.

(3) Salem, L. *Electrons in Chemical Reactions: First Principles*; Wiley, New York, 1982.

(4) Tully, J. C.; Preston, R. K. *J. Am. Chem. Soc.* **1971**, *55*, 562.

(5) (a) Von Neumann, J.; Wigner, E. *Phys. Z.* **1929**, *30*, 467. (b) Teller, E. *J. Phys. Chem.* **1937**, *41*, 109. (c) Herzberg, G.; Longuet-Higgins, H. C. *Trans. Faraday Soc.* **1963**, *35*, 77. (d) Herzberg, G. *The Electronic Spectra of Polyatomic Molecules*; Van Nostrand: Princeton, NJ, 1966, p 442. (e) Mead, C. A.; Truhlar, D. G. *J. Chem. Phys.* **1979**, *70*, 2284. (f) Mead, C. A. *Chem. Phys.* **1980**, *49*, 23. (g) Keating, S. P.; Mead, C. A. *J. Chem. Phys.* **1985**, *82*, 5102. (h) Keating, S. P.; Mead, C. A. *J. Chem. Phys.* **1987**, *86*, 2152.

(6) Bernardi, F.; Olivucci, M.; McDouall, J. J. W.; Robb, M. A. *J. Chem. Phys.* **1988**, *89*, 6365.

(7) McWeeny, R.; Sutcliffe, B. *Methods of Quantum Mechanics*; Academic: New York, 1969.

(8) Eyring, H.; Walter, J.; Kimball, G. *Quantum Chemistry*; Wiley: New York, 1944.

0002-7863/90/1512-1737$02.50/0